Structural Diversity of Occluding Junctions in the Low-resistance Chloride-secreting Opercular Epithelium of Seawater-adapted Killifish (Fundulus heteroclitus)

STEPHEN A. ERNST, WILLIAM C. DODSON, and KARL J. KARNAKY, JR.

Department of Anatomy, University of Michigan, Medical Sciences II, Ann Arbor, Michigan 48109;
Department of Anatomy, Temple University School of Medicine, Philadelphia, Pennsylvania 19140; and
the Mount Desert Island Biological Laboratory, Salsbury Cove, Maine 04672

ABSTRACT The structural features of the chloride-secreting opercular epithelium of seawater-adapted killifish (Fundulus heteroclitus) were examined by thin-section and freeze-fracture electron microscopy, with particular emphasis on the morphological appearance of occluding junctions. This epithelium is a flat sheet consisting predominantly of groups of mitochondria-rich chloride cells with their apices associated to form apical crypts. These multicellular groups are interspersed in an otherwise continuous pavement cell epithelial lining. The epithelium may be mounted in Ussing-type chambers, which allow ready access to mucosal and serosal solutions and measurement of electrical properties. The mean short-circuit current, potential difference (mucosal-side negative), and DC resistance for 19 opercular epithelia were, respectively, $120.0 \pm 18.2 \ \mu A/cm^2$, 12.3 ± 1.7 mV, and $132.5 \pm 26.4 \ \Omega cm^2$. Short-circuit current, a direct measure of Cl^- transport, was inhibited by ouabain ($5 \ \mu m$) when introduced on the serosal side, but not when applied to the mucosal side alone. Autoradiographic analysis of [3H]-ouabain-binding sites demonstrated that Na^+,K^+-ATPase was localized exclusively to basolateral membranes of chloride cells; pavement cells were unlabeled. Occluding junctions between adjacent chloride cells were remarkably shallow (20-25 nm), consisting of two parallel and juxtaposed junctional strands. Junctional interactions between pavement cells or between pavement cells and chloride cells were considerably more elaborate, extending 0.3-0.5 μm in depth and consisting of five or more interlocking junctional strands. Chloride cells at the lateral margins of crypts make simple junctional contacts with neighboring chloride cells and extensive junctions with contiguous pavement cells. Accordingly, in this heterogeneous epithelium, only junctions between Na^+,K^+-ATPase-rich chloride cells are shallow. Apical crypts may serve, therefore, as focal areas of high cation conductivity across the junctional route. This view is consistent with the electrical data showing that transmural resistance across the opercular epithelium is low, and with recent studies demonstrating that transepithelial Na^+ fluxes are passive. The simplicity of these junctions parallels that described recently for secretory cells of avian salt gland (Riddle and Ernst, 1979, J. Membr. Biol., 45:21-35) and elasmobranch rectal gland (Ernst et al., 1979, J. Cell Biol., 83:(2, Pt. 2):83 a[Abstr.]) and lends morphological support to the concept that paracellular ion permeation plays a central role in ouabain-sensitive transepithelial NaCl secretion.

Although ouabain-sensitive Na^+ pumps appear to play a crucial role in transepithelial salt secretion, the unexpected but consistently observed subcellular localization of this enzyme to the inward-facing basolateral plasma membranes of secretory cells (13, 22, 23) is perplexing. Recently, several laboratories have rationalized this apparent contradiction by proposing a

model for salt secretion in which intercellular space Na$^+$, generated by basolateral plasmalemmal Na$^+$,K$^+$-ATPase, enters the luminal compartment across the zonula occludens ("tight" junction) in response to a favorable electrical potential derived from secondary "active" transcellular transport of Cl$^-$ (21, 25, 49, 50). This model is predicated in part on the presence of a high conductance cation-selective shunt pathway across the zonula occludens. Accordingly, Riddle and Ernst (45) examined occluding junctions in avian salt gland secretory epithelium by thin-section and freeze-fracture electron microscopy and found them to exhibit a morphological simplicity resembling that described for several absorptive epithelia known to be leaky to ions (4, 5).

Although the presence of structurally simple junctions in salt-gland epithelium is consistent with the proposed secretory transport model, this support remains somewhat circumstantial inasmuch as histological restraints preclude critical measurements of electrical parameters across this epithelium. Recently, Karnaky and collaborators (6, 36, 38) introduced the teleost opercular epithelium as a model system for studying salt secretion (reviewed by Karnaky [35]). This model system joins a small but growing list (cf. Frizzell et al. [27]) of chloride-secreting epithelia that can be mounted in modified Ussing chambers for electrophysiological study. Like the teleost branchial epithelium with which it is structurally and functionally analogous, the opercular epithelium consists of a heterogeneous cell population of ion-transporting chloride cells and nontransporting pavement cells and mucous cells. In the present study of opercular epithelia from seawater-adapted *Fundulus heteroclitus*, we describe the simplicity of occluding junctions between transporting chloride cells, in contrast to the extensive junctions between pavement cells, and suggest that the observed junctional architecture between chloride cells is consistent with the observation that transmural resistances measured across in vitro preparations are quite low, as might be expected if these junctions exhibit a high conductivity for cations. In addition, we show the selective localization of Na$^+$ pumps to the basolateral plasmalemmal surfaces of chloride cells in this epithelium and establish the sensitivity of short-circuit current and transepithelial potential (seawater-side negative) to ouabain following serosal, but not to mucosal only, exposure to the inhibitor. A preliminary account of this work was presented (18).

MATERIALS AND METHODS

Animals

Euryhaline killifish, *Fundulus heteroclitus*, weighing 4–12 g were purchased at a local bait shop and adapted for 2–4 wk to artificial seawater (Utility Seven Seas Mix, Utility Chemical Co., Paterson, N. J.) in aerated aquaria at 21–25°C, following the technique of Karnaky et al. (37). Dry fish food was provided at least twice weekly during adaptation.

Electrical Studies

Animals were sacrificed by pithing and decapitation. The opercula were spread laterally under a fish Ringer's solution (6) to expose the inner mucosal lining. The epithelium was then teased free from the underlying opercular bone with fine forceps, as described in detail by Karnaky and Kinter (38), and mounted in lucite chambers (6, 36). Short-circuit current (I_{sc}) and open-circuited potential difference (PD) were determined following the methods of Degnan et al. (6). Transepithelial DC resistance (R) was estimated as the ratio of PD to I_{sc}.

Ouabain Binding Studies

The effects of 5 μm ouabain on I_{sc} and PD across opercular skins were monitored after addition of the glycoside to only the mucosal, or to only the serosal, Ringer's solutions. Irreversibility of the inhibitory effect of ouabain on these electrical parameters was assessed during repeated washes of the mounted skins with Ringer's solution. For autoradiographic localization of [^{3}H]ouabain-binding sites (cf. Ernst and Mills [21, 22]), opercula were exposed for 60 min to mucosal plus serosal ouabain solutions containing 12 μCi/ml of [^{3}H]ouabain (specific activity of 12 Ci/mmol), washed for 30 min, and then rapidly frozen in Freon cooled to liquid nitrogen temperature. The frozen tissue was then freeze-dried in a Stumpf-Roth freeze-dry apparatus (Thermovac Industries Corp., Copaigue, N. Y.), vapor-fixed with OsO$_4$ under vacuum, and embedded in low viscosity Spurr resin (Electron Microscopy Sciences, Fort Washington, Pa.) as described previously (21). Sections (1-μm thick) were coated with NTB-2 emulsion (Eastman Kodak Co., Rochester, N. Y.) and processed for autoradiography (21).

Morphological Studies

Opercular epithelia were exposed to fixative either *in situ* or immediately after removal from the opercular bone. For conventional electron microscopy, tissue was fixed in Ringer's solution containing 6% glutaraldehyde for 90 min at room temperature, washed in Ringer's, and postfixed for 90 min in 1% OsO$_4$ in 0.1 M cacodylate, pH 7.4. To enhance membrane contrast, some of the osmicated tissue was incubated for 15 min in 1% tannic acid solution (Mallinkrodt, Inc., St. Louis, Mo.) in 0.1 M cacodylate, pH 6.8 (51). After rinsing in distilled water, tissues were dehydrated and embedded in Spurr resin. Thin sections were double stained with uranyl acetate and lead citrate.

For freeze-fracture studies, opercula were fixed for 30 min in Ringer's solution containing 3% glutaraldehyde, rinsed with Ringer's, and then infiltrated for from 90 min to several weeks in 25% glycerol in Ringer's. Narrow strips of opercular skin were rolled into a "jelly roll", transferred to gold supports, and frozen in Freon 22 cooled in liquid nitrogen. Freeze-fractured replicas were prepared in Balzers 301 or 360 M instruments (Balzers Corp., Nashua, N. H.), each equipped with a platinum-carbon gun and a quartz crystal monitor. The temperature of tissue before fracturing was −112°C. The replicas were cleaned by sequential exposure to Chlorox and to sulfuric acid-dichromate solutions, rinsed in distilled water, picked up on uncoated grids, and viewed with Philips 201 and 300 electron microscopes.

RESULTS

Histology of Opercular Epithelium from Seawater-adapted Killifish

The histological organization of opercular epithelium was described previously (38) and is reviewed here briefly for purposes of orientation. The opercular mucosa faces the gill chamber and may be teased free from the underlying opercular bone (Fig. 1). The opercular epithelium rests on a basal lamina and is supported by underlying loose connective tissue containing a rich vascular supply. The epithelium is characterized by a heterogeneous cell population, which includes a squamous pavement cell lining, chloride cells, occasional mucous cells, and supportive or undifferentiated cells. In seawater-adapted fish, the mitochondria-rich chloride cells extend from the basal lamina to the external environment where their apices associate to form characteristic apical crypts circumscribed by the contiguous pavement cell lining (Fig. 1). The histological organization is similar to that of the gill epithelium with the notable exception that the opercular epithelium lacks respiratory leaflets (38).

Whereas the density of chloride cells in the *Fundulus* gill is as low as 6% (39), the density in opercular epithelium may be as high as 50% (38). However, examination of 1-μm–thick sections of opercular skin or of living wholemounts under phase contrast microscopy or fluorescence microscopy after vital staining with the mitochondrial fluorescent probe, dimethylaminostryrylmethylpyridiniumiodide (2), indicates that chloride cells are grouped into areas of low density and high density within the same skin (data not presented). In general, chloride cell-rich regions could be recognized, even under the
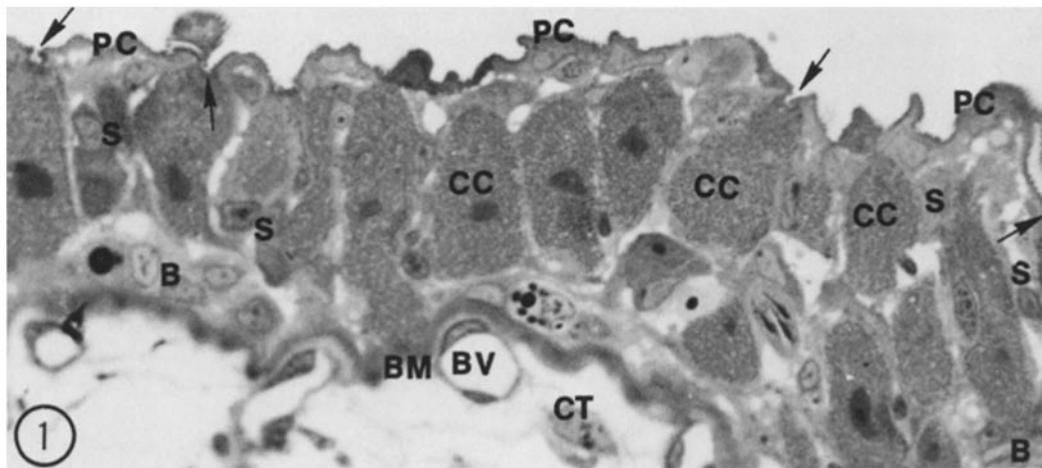
FIGURE 1 This light micrograph illustrates the morphological features of the opercular epithelium. The opercular mucosa has been teased free from the underlying opercular bone as a flat sheet. The epithelium is covered by a thin lining of squamous pavement cells (PC). Mitochondria-rich chloride cells (CC) rest on a basement membrane (BM), and their free surfaces, when included in the plane of section, form apical crypts (arrows) that are exposed to the external seawater environment. Undifferentiated supporting cells (S) are present between chloride cells and basal cells (B) are found adjacent to the basement membrane. Neither cell type has luminal exposure. The serosal connective tissue (CT) contains many blood vessels (BV) closely associated with the overlying epithelium. × 800.

dissecting microscope, because they corresponded invariably to areas of differentially high vascularity. Samples of opercular skin used in the present study were generally taken from these chloride cell-rich areas.

Electrical Studies

Opercular epithelia, mounted in lucite chambers and bathed on both sides with normal Ringer's solution, generate a spontaneous PD (seawater-side negative) and I_{sc}, which climb to a steady state within about 40 min (Fig. 2). To establish control values, the I_{sc} and PD were determined at 20-min intervals over the next hour and averaged (6). During this control period, the I_{sc} typically exhibited a decay rate of ~5%/h. The mean I_{sc}, PD, and DC resistance for the 19 opercular epithelia used in the present study were, respectively, $120.0 \pm 18.2 \ \mu A/cm^2$, 12.3 ± 1.7 mV, and $132.5 \pm 26.4 \ \Omega cm^2$. The transmural resistance falls at the lower end of the range of epithelia which are classified as "leaky" (4, 5, 10).

As shown in Fig. 2 and Table I, an 80-min exposure to 5 μm ouabain on only the serosal side resulted in a statistically significant decline in I_{sc} and PD. The difference between the mean percent decline in I_{sc} ($51.3 \pm 8.6\%$) and the mean precent decline in PD ($66.7 \pm 5.9\%$) was not statistically significant. The inhibitory effects of this exposure were not reversed by repeated washing with ouabain-free Ringer's solution. Exposure to 5 μM ouabain on only the mucosal side had no significant effect on I_{sc} or PD (Table I).

Autoradiographic Localization of [^{3}H]Ouabain-binding Sites

The autoradiographic distribution of [^{3}H]ouabain-binding sites in opercular epithelium after mucosal plus serosal exposure to ouabain is shown in Figs. 3 and 4. Chloride cells were heavily labeled, whereas pavement cells and supportive cells did not bind ouabain appreciably. The apparent intracellular localization of binding sites is caused by tubular invaginations of Na^+,K^+-ATPase-rich basolateral plasmalemma into the in-
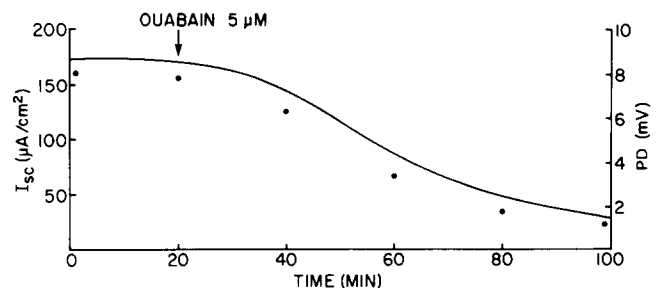
FIGURE 2 The inhibitory effects of 5 μM ouabain (serosal exposure) on electrical properties of an isolated opercular epithelium mounted between lucite chambers are shown. The epithelium was bathed on both sides with Ringers' solution. The curve is the continuous short-circuit current (I_{sc}) recording and the dots are the spontaneous open-circuited potential difference (PD) measurements.

terior of chloride cells (see below). Note the absence of silver grains over nuclei. In addition to the differential cell specificity of ouabain binding, membrane specificity is demonstrated by the absence of Na^+ pump sites along the outward-facing surfaces of chloride cells that border apical crypts (Figs. 3 and 4). Labeling above background levels was abolished by the addition of 10^{-4} M unlabeled ouabain to the incubation medium.

Fine Structure of Opercular Epithelium

Fig. 5 illustrates the salient features of opercular epithelial ultrastructure. The free surfaces of the squamous pavement cells are plicated and exhibit a thick glycocalyx. The cytoplasm is granular and contains abundant microfilaments and tonofilaments, as well as occasional profiles of rough endoplasmic reticulum, electron-dense granules, and mitochondria. In contrast, chloride cells are characterized by numerous mitochondria that are closely associated with tubular extensions of the basolateral plasmalemmal surface. Several chloride cells interdigitate with one another, and their free surfaces form glycoprotein-rich apical crypts that lie deep to the pavement epithe-

lial sheet but maintain their continuity with the external environment through apical pores (Fig. 5). Apical crypts are shared generally by chloride cells and a chloride cell variant, which is characterized by fewer mitochondria and a less extensive tubular reticulum. This cell type, termed accessory cell, was described in teleost pseudobranch epithelium (15) and gill epithelium (33, 34, 47). In the operculum, images from thin sections of apical crypts suggest that accessory cells commonly interdigitate with chloride cells (Fig. 5). A similar conclusion was reached for the branchial epithelium of several seawater-adapted teleosts (34, 47).

TABLE I

Effects of an 80-min Exposure to 5 μM Ouabain on the Electrical Properties of Isolated, Short-circuited Opercular Epithelia of Seawater-adapted F. heteroclitus

	I_{sc}*	PD	R
	$\mu A/cm^2$	mV	$\Omega\text{-}cm^2$
Control (7)	117.5 ± 40.4	11.3 ± 4.0	147.7 ± 64.6
Mucosal exposure	118.7 ± 41.5	11.0 ± 3.6	117.5 ± 84.0
P	NS	NS	NS
Control (7)	133.3 ± 30.9	10.8 ± 2.5	101.9 ± 30.5
Serosal exposure	77.1 ± 25.5	3.8 ± 1.3	103.6 ± 41.9
P	<0.005	<0.005	NS

For each electrical property, the average of four control period values are compared with the value 80 min after introduction of the drug. Results are expressed as mean ± SEM and the number of experiments is given in parentheses. Statistical analyses were by *t* test for matched pairs (two-tailed). Statistical significance was taken at P < 0.05. NS denotes lack of significance. Data are from epithelia gassed with 95% O_2/5% CO_2.

* Corrected for 5%/h decay rate observed during the control period.

Structural Features of Occluding Junctions in Opercular Epithelium

Contiguous pavement cells are joined near their free surfaces by zonulae occludentes. In thin sections, these junctions are extensive in their apical to basal extent (Fig. 5) and at high magification (Fig. 6) appear as an area of fusion between outer plasmalemmal leaflets with a total junctional depth of 0.3–0.5 μm. A unique feature of this junction, which to our knowledge has not been described previously, is the presence of an electron-dense plaque on either side of the zonula occludens near the apical border. These plaques are present in published images of pavement cells from gills (e.g., Fig. 2 a in reference 47). The plaque is not associated generally with cytoplasmic filaments. Desmosomal contacts with associated tonofibrils are seen commonly between lateral plasmalemmal surfaces (Figs. 5 and 6).

The extensive nature of the pavement cell-payment cell junctions is reflected in freeze-fracture images where the junctions are presented as an anastomosing network of junctional strands on the P-fracture face and corresponding grooves on the E face (Fig. 7). Junctions between pavement cells and occasional mucous cells are also elaborate (Fig. 7). These junctions usually consist of five to eight strands and encompass an average junctional depth of 0.5 μm. Gap junctions were seen occasionally as small focal accumulations of intramembrane particles on P-fracture faces between pavement cell lateral membranes. Gap junctions associated with chloride cells were not observed. P- and E-fracture faces of the apical plasma membrane of pavement cells bear few intramembrane particles. No evidence of particle aggregation was observed along these cleaved surfaces, in contrast to the observations of Sardet et al. (47), on pavement cells in gill epithelium.
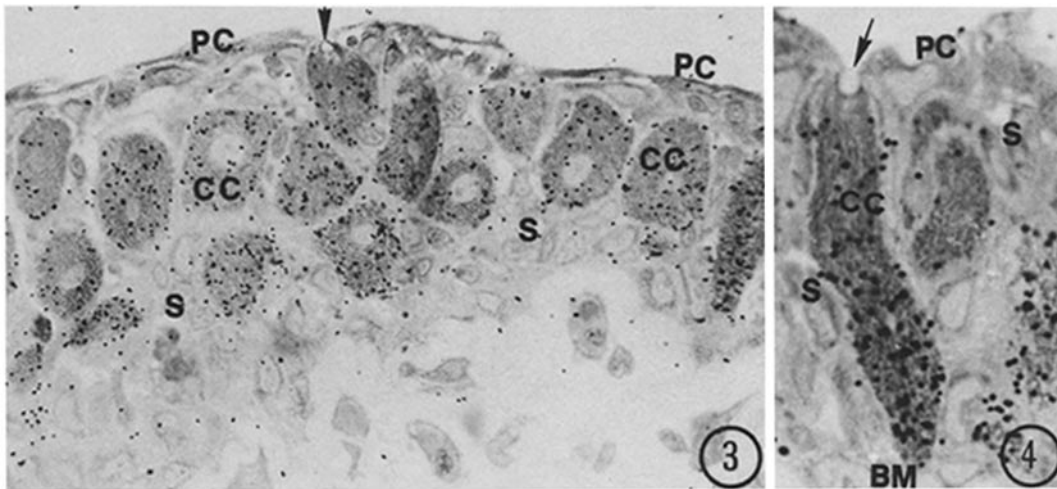
FIGURE 3 This autoradiograph shows the distribution of [³H]ouabain-binding sites in a tangential section from an isolated opercular epithelium. The tissue was exposed for 60 min at 25°C on both mucosal and serosal surfaces to 1 μM ouabain containing 12 μCi/ml of [³H]ouabain, and then washed for 30 min in isotope-free Ringer's solution. Mitochondria-rich chloride cells (CC) are heavily labeled, whereas pavement cells (PC) and supporting cells (S) do not bind ouabain above background levels. The apparent intracellular localization of binding sites is caused by tubular extensions of the basolateral plasmalemma (see Fig. 5); note the absence of silver grains over nuclei. Apical surfaces of chloride cells bordering an apical crypt (arrow) are unlabeled. 1-μm-thick section of freeze-dried, plastic-embedded tissue, coated with NTB-2 emulsion and exposed for 7 d. × 1,200.

FIGURE 4 Autoradiograph of opercular epithelium after exposure to [³H]ouabain as in Fig. 3. A chloride cell (CC) is seen extending from the basement membrane (BM) to the free surface of the epithelium. Despite the direction of net NaCl transport from the blood side to the seawater side of the epithelium, ouabain-binding sites are present on the inward-facing (tubular extensions of the) basolateral membranes of the chloride cell and are absent from the free surface at the apical crypt (arrow). Pavement cells (PC) and supporting cells (S) also do not bind [³H]ouabain. Portions of three other chloride cells are present in this micrograph, one of which appears only lightly labeled. × 1,400.
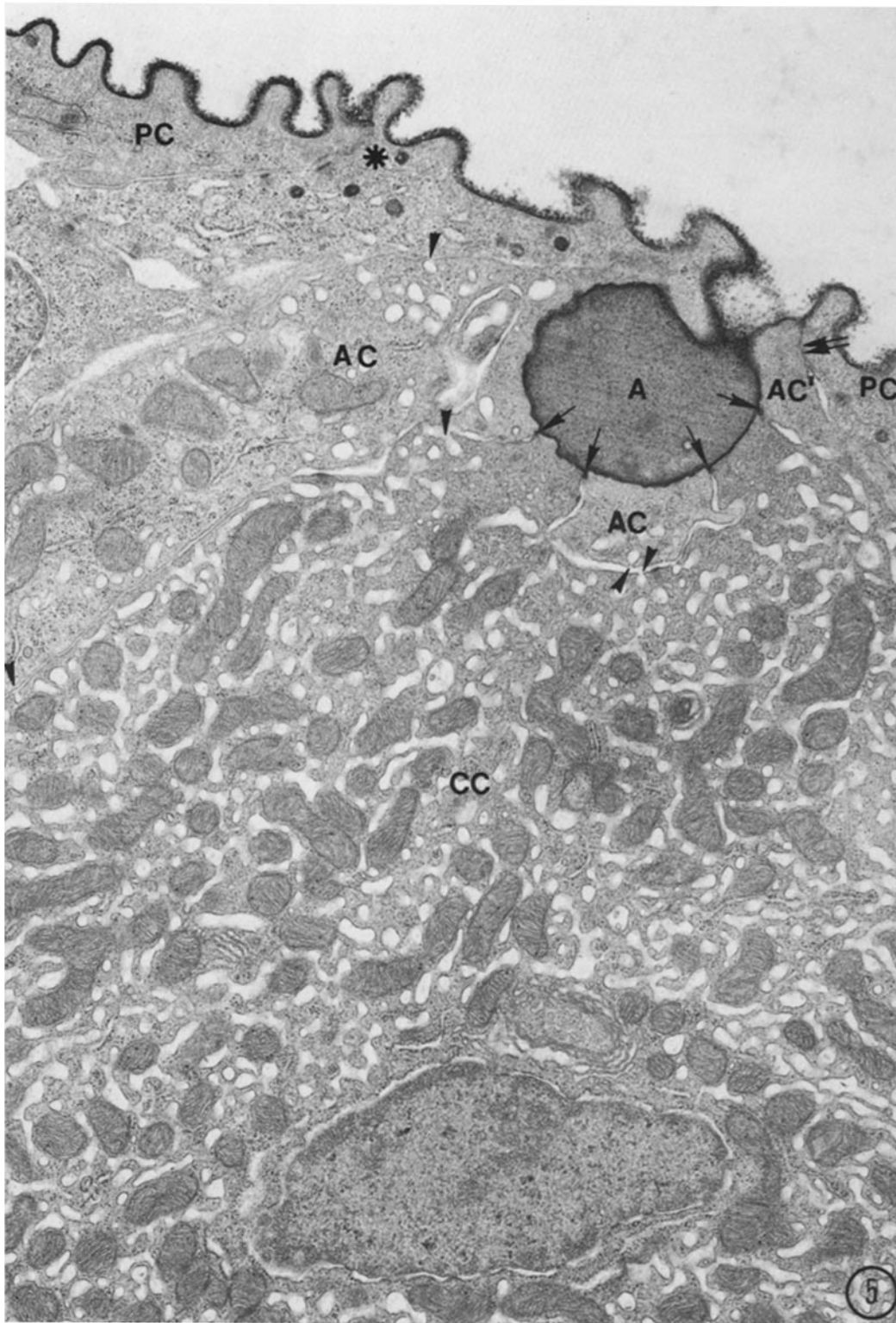
FIGURE 5 The opercular muscosa is covered by squamous pavement cells (PC) which have their carbohydrate-rich plicated surfaces exposed to the external seawater environment. Chloride cells (CC) are characterized by abundant mitochondria and by an extensive anastomosing reticulum which is formed by tubular extensions of (Na^+,K^+-ATPase-rich) basolateral plasmalemma. Patency between tubular lumina and intercellular spaces is shown (arrowheads). Chloride cells are grouped in multicellular complexes with their narrow, interdigitating apices defining an apical crypt (A), also in contact with seawater. Commonly, such interdigitations occur between chloride cells (CC) and a chloride cell variant (accessory cell, AC) that exhibits fewer mitochondria and a less-developed tubular reticulum. Occluding junctions between these cells are invariably shallow (arrows). In contrast, junctions between chloride or accessory cells and pavement cells at the lateral edges of crypts (double arrows), and those between adjacent pavement cells (asterisk), are well developed. Note that the portion of accessory cell labeled AC' makes a shallow junctional contact with an adjacent chloride cell (arrow), as well as an extensive contact with a neighboring pavement cell (double arrow). Tannic acid fixation. × 17,500.
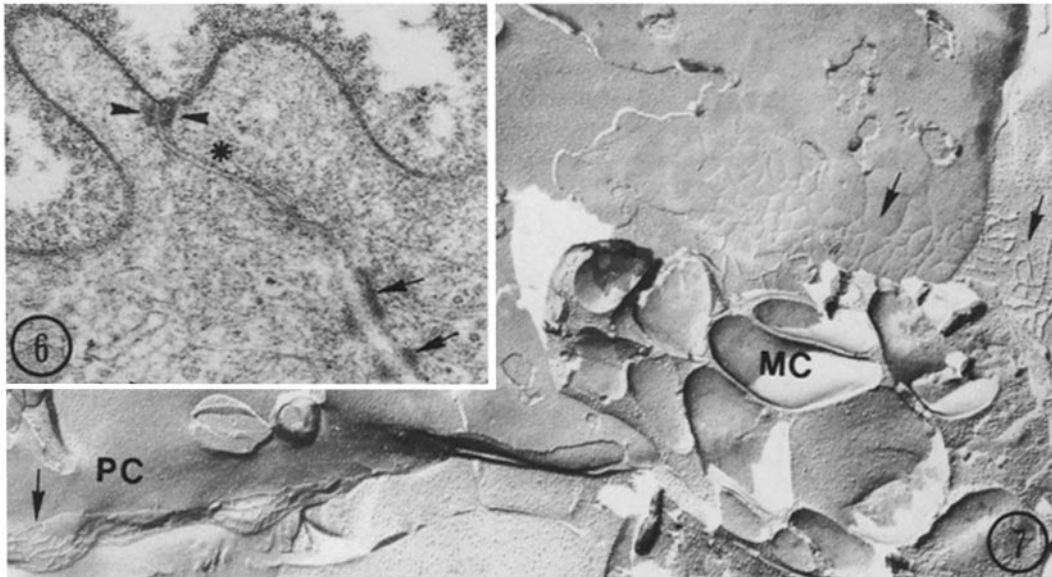
FIGURE 6   The zonula occludens between pavement cells is extensive (asterisk), extending 0.3–0.5 μm in depth. A dense plaque is seen characteristically on the cytoplasmic sides of the occluding junction near the apical border (arrowheads). Desmosomes are present deep to the occluding junction (arrows), where they appear with characteristic plasmalemmal plaques associated with tonofibrils but without a central density in the extracellular space. Tannic acid, included in the fixation protocol, enhances membrane contrast and the glycoprotein coat of the free surface of the epithelium. × 57,000.

FIGURE 7   This freeze-fracture replica shows the extensive barriers, in the form of anastomosing strands and grooves (arrows), which characterized occluding junctions between neighboring pavement cells (PC) or between pavement cells and the occasional mucous cell (MC) that appears singly along the epithelial border. × 19,000.

The region of the apical crypt is shown in Figs. 5 and 8. In contrast to the extensive junctions between pavement cells, occluding junctions between neighboring chloride cells are remarkably simple in their extent. Transverse thin sections of these junctions (Fig. 5) and cross-fractured images (Fig. 8) suggest that these junctions consist of a single focal contact. When viewed in the plane of the membrane with freeze-fracture, these junctions are revealed as doublets ~20–25 nm in width. Each doublet appears as two closely juxtaposed parallel strands when the fracture passes from the P face of the lateral membrane of the cell to the P face of its luminal membrane (Fig. 9), and two parallel grooves when the complementary E faces are viewed (Fig. 8). The junction often appears as a single strand when the fracture makes the more common transition from the E face of the lateral membrane to the P face of the luminal membrane of an adjacent cell (Fig. 10). However, close examination of these fractures reveals that the replicated surfaces include a groove on the E face and a ridge on the P face (Fig. 10). The close apposition of the doubtlet strands often makes the groove difficult to resolve. Similar observations were made on doublet junctional strands in salt-gland epithelium (45).

The third major type of junctional interaction is that between chloride cell and pavement cell at the lateral borders of the apical crypts. As demonstrated in thin sections, these contacts are invariably extensive (Fig. 5), extending 0.3–0.5 μm in depth. A remarkable feature of chloride cell junctional specialization is the observation that a single chloride cell may make elaborate contact with a pavement cell and a simple contact with a neighboring chloride cell or accessory cell (Fig. 5).

DISCUSSION

Physiological data derived exclusively from studies of ion absorbing epithelia have demonstrated that occluding junctions

in some epithelia are leaky, thereby providing a paracellular route for ion permeation (3, 28–30). In general, leaky epithelia exhibit low transmural resistances coupled with high osmotic water permeabilities and shallow solute gradients generated by active transport; tight epithelia demonstrate the opposite properties (10, 30). Accordingly, low-resistance epithelia generally elaborate isotonic absorbates, whereas tight epithelia function in the production of hypertonic fluids. Claude and Goodenough (5) and Claude (4) demonstrated a close correlation between the number of junctional strands seen in freeze-fracture images of occluding junctions and junctional tightness, as judged by transmural resistance values. Specifically, with the exception of the rat distal tubule (41), resistance values for hypertonic absorptive epithelia, such as the rabbit collecting tubule (32), the toad urinary bladder, and the frog skin (17), fall toward the high end of the wide range exhibited by absorptive epithelia. All of these hypertonic absorptive epithelia exhibit a relatively larger number of junctional strands when compared with leaky isotonic absorptive epithelia, such as renal proximal tubules and gall bladder (4, 5, 44). Based on freeze-fracture data describing morphologically simple junctions between salt-secretory cells in avian salt gland (16, 45) and, in the present study, in killifish opercular epithelium, a radically different picture is emerging concerning the structure of the zonula occludens in epthelia that function in hypertonic secretion.

An early model for hypertonic NaCl secretion across gill epithelium (40) proposed that Na^+ and Cl^- were transported solely through transcellular pathways involving active transport carriers at the apical membrane: Na^+ by Na^+,K^+-ATPase and Cl^- by an electrogenic pump. Although circumstantial evidence for apical Na^+,K^+-ATPase in the teleost chloride cell initially seemed compelling, more recent physiological and biochemical studies in teleosts challenged the original interpre-

tation of these experiments (reviewed by Karnaky [35]), and cytochemical and autoradiographic studies showed directly that most, if not all, of the Na^+,K^+-ATPase of gill chloride cells is located at the basolateral cell surface (33, 39). Indeed, Na^+,K^+-ATPase was found to be predominantly basolateral in all hypertonic secretory epithelia examined to date (13, 22, 23), thus showing, paradoxically, the same localization as that in absorptive epithelia. Equally puzzling was the observation that zonulae occludentes between hypertonic secretory cells of several epithelia were permeated by colloidal lanthanum solutions (42, 47, 53). When considered from the perspective that active Cl^- transport in a number of secretory tissues is inhibited by serosal ouabain and is dependent on the presence of Na^+ (data summarized by Frizzell et al. [27]), the nonluminal location of Na^+ transport sites stimulated several investigators to suggest a new hypothesis for salt secretion that includes paracellular and transcellular routes for ion movements. This concept was presented for secretory epithelia in general (25) and for several hypertonic secretory tissues including the teleost gill chloride cell (49), the avian salt gland (21, 45), and the elasmobranch rectal gland (50, 52). This model, modified to incorporate the present data for the opercular epithelium, is described in Fig. 11.

This hypothesis, which explains how a primary active transport process (Na^+,K^+-ATPase) plays a role in secondary Cl^- secretory transport, is consistent with a growing body of data gathered from physiological experiments with gills and rectal glands (14, 24, 49, 50, 52). The aggregate data on ion transport across the opercular epithelium provide strong support for this secretory model by correlating in a single hypertonic secretory epithelium evidence for ouabain-sensitive "active" Cl^- transport, passive Na^+ fluxes, a cation-selective shunt pathway, and a morphological basis for paracellular Na^+ movement. Thus, active Cl^- transport was demonstrated definitively under short-circuit conditions and was shown to be dependent on the presence of Na^+ and Cl^- in the bathing medium and to be reduced by ouabain or furosemide (6, 36). In contrast, Na^+ fluxes under either short-circuited or open-circuited conditions behave passively (6–8) and the transepithelial potential measured in seawater approximates the Na^+ equilibrium potential (9). Recently, Degnan and Zadunaisky (8) demonstrated that bidirectional Na^+ fluxes across the opercular epithelium could be blocked by triaminopyrimidine (TAP), a compound that blocks the cation-selective shunt pathway in absorptive epithelia (43). These data, together with the evidence for the passive nature of the Na^+ flux, although not conclusive, are consistent with the proposed presence of a cation-specific paracellular

pathway across the epithelium. The present study demonstrates that the operculum maintains a very low transmural resistance (132.5 Ωcm^2), as would be expected if the epithelium exhibits a highly conductive cation permeable channel, and reveals that the zonulae occludentes between adjacent chloride cells are

SEAWATER 470 Na⁺
560 Cl⁻
10 K⁺
-15 p.d.

INTERNAL 150 Na⁺
140 Cl⁻
3 K⁺
0 p.d.
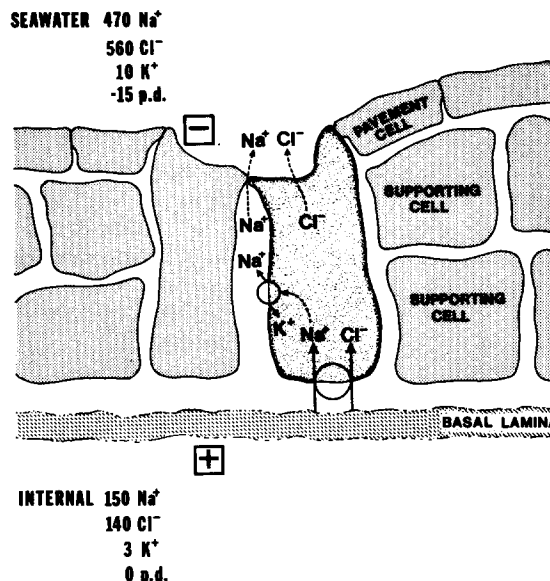
FIGURE 11 This diagram is a schematic model for the secretory movement of Na^+ and Cl^- across the opercular epithelium of seawater-adapted killifish. Values for PD (millivolts) and electrolyte concentrations (milliequivalents per liter) in seawater (mucosal) and internal (serosal) compartments are given above and below the epithelium, respectively. Pavement cells are joined to each other and to chloride cells at the lateral margins of apical crypts by extensive junctions. Junctions between neighboring chloride cells within the crypt are invariably shallow. The interdigitation of two or more chloride cells to form a single apical crypt increases the linear amount of junction available for paracellular transport per square centimeter of apical surface. Chloride is transported initially into chloride cells from the blood side by a Na^+-facilitated, neutral-coupled carrier at the basolateral interface. This secondary "active" transport is driven by the low intracellular Na^+ gradient established by the primary active transport of Na^+ out of the cell by basolateral plasmalemmal Na^+,K^+-ATPase. Chloride crosses the luminal membrane by passive electrical forces, whereas intercellular space Na^+ gains the luminal space via the paracellular route between chloride cells, driven by the negative potential established by Cl^- movement. In the operculum, apical crypts would represent focal areas of low transmural resistance associated with Na^+,K^+-ATPase-rich chloride cells.

FIGURE 8 This micrograph shows a freeze-fracture replica of an apical crypt. The apical crypt is shared by several chloride cells joined at their apices by occluding junctions that appear shallow when viewed in cross-fracture (arrows). A portion of the particle-rich luminal E fracture face (EF) of a chloride cell is shown separated from the particle-poor E face (E) of the lateral membrane by two closely apposed parallel grooves (arrowhead). A portion of the more extensive junction between chloride cell and pavement cell (PC) at the lateral margin of the crypt is shown at the lower left (asterisk). Apical vesicles and tubules are often present in the apical cytoplasm. X 40,500.

FIGURE 9 When the fracture plane passes from the P face of the apical membrane of a chloride cell (PF) to the P face of its lateral membrane (P), the occluding junction is revealed as a doublet consisting of two parallel strands that are closely juxtaposed (20–25 nm total width). X 110,000.

FIGURE 10 When the fracture passes from the P face (PF) of the luminal membrane of a chloride cell to the E face (E) of the lateral membrane of an adjacent chloride cell, the transition produces a strand on the P face (arrow) and a groove on the E face (arrowhead). A portion of P face lateral membrane (P) is also shown, revealing the doublet nature of the junction (apposing arrows). X 100,000.

shallow (Figs. 5 and 8), consisting of two junctional strands (Figs. 8–10). Furthermore, consistent with the neutral-coupled NaCl carrier model, short-circuit current is not inhibited by exposure to mucosal ouabain (Table I) and Na^+,K^+-ATPase is predominantly localized to the basolateral (tubular extensions) of the plasma membranes of chloride cells, even when [^3H]-ouabain was included in both mucosal and serosal compartments (Figs. 3 and 4). The apparent abundance of binding sites associated with chloride cells might reflect the extensiveness of the basolateral plasma membrane rather than a higher density of Na^+ pump sites per unit surface area. If this were the case, pavement cells might have a similar density of pump sites, although their absolute number might be too few to be resolved with the autoradiographic procedure. However, this seems unlikely because Na^+,K^+-ATPase activity, when resolved cytochemically in gill epithelium (33), is localized predominantly to chloride cells; pavement cells have little activity despite the amplification of enzymatic activity by accumulation of reaction product over time of incubation with substrate.

On the basis of these data, we propose that the morphological basis for the low resistance of the opercular epithelium is related to the simple chloride cell-chloride cell junctional interactions. Moreover, interdigitation of chloride cells at their narrow apices (Figs. 5 and 8) increases the tortuosity of the intercellular junctions, a factor that is critical to calculations of the specific resistance of paracellular pathways (4). The overall result is a maximization of the linear amount of junction available for ionic conductance per square centimeter of luminal surface.[1] Shallow junctions occur only between chloride cells, or between chloride cells and the chloride cell variant, the accessory cell (34, 47; see Fig. 5), and are specifically confined, therefore, to the apical crypts (Figs. 5 and 8) which are characteristic of the opercular epithelium (and branchial epithelium) of seawater-adapted fish. Junctions shared by pavement cells and chloride cells or by adjacent pavement cells, which constitute the major epithelial barrier to seawater, are considerably more elaborate, extending 0.3–0.5 mm in depth (Figs. 5 and 6) and consisting of five or more interlocking strands (Fig. 7). Considered in this light, the diversity of junctional interactions may provide for focal areas of high ionic conductance (i.e., apical crypts) intimately associated with Na^+,K^+-ATPase-rich chloride cells (Figs. 3 and 4) in an epithelium otherwise characterized by extensive junctional contacts (see Fig. 11). Definitive data concerning a high conductance junctional route between chloride cells await use of cable analysis or voltage scanning techniques of the type performed by Fromter (29) in leaky gallbladder epithelium. Although it is not yet possible to measure directly electrical parameters across the teleost branchial epithelium because of the complex histology of this tissue, Sardet et al. (47) showed that chloride cells and pavement cells in gills possess a junctional morphology similar to that described here for the operculum.

The present data, although entirely compatible with the secretory scheme presented in Fig. 11, do not provide information on an additional requisite of chloride cell junctions that is essential to the model. Not only must the junctions be cation specific, but for efficient hypertonic secretion they must be relatively impermeable to water. Whereas there is considerable precedence in the literature for differential junctional perme-

ability to Na^+ over Cl^- in leaky absorptive epithelia (1, 11, 43) and suggestive evidence in the operculum (7–9), the routes of transepithelial water movement remain poorly characterized for almost all epithelia (11, 12). Although many investigators consider that a highly conductive paracellular route for passive ion permeation would contribute substantially to the total osmotic water flux across low-resistance epithelia (31, 46, 48), there is also evidence that suggests that water flux may be primarily transcellular (12, 26, 54). It is clear, however, that the secretory model depicted in Fig. 11 would be compromised seriously if junctional cation conductance in epithelia proves to be necessarily accompanied by leakiness to osmotic water flow.

It is apparent from the recent physiological and morphological data on secretory epithelia discussed above that NaCl movement across tissues in this class of transporting epithelia cannot be explained by models that posit only transcellular pathways. In the four hypertonic secretory epithelia that have been examined to date, teleost opercular epithelium (present work), branchial epithelium (47), avian salt gland (45) and elasmobranch rectal gland[2] (20), thin-section and freeze-fracture electron microscopy reveal that transporting cells are joined at their apical poles by shallow junctions that resemble those of leaky ion-absorptive epithelia. Moreover, junctions in all of these secretory epithelia are characterized uniquely by a few closely juxtaposed and parallel junctional strands between the Na^+,K^+-ATPase-rich secretory cells. These contrast with the commonly observed anastomosing network seen between most absorptive epithelial cells (4, 5) and between those cells in secretory epithelia that are not specialized morphologically for transepithelial transport and are unreactive for Na^+,K^+-ATPase activity (cf. reference 45 and Figs. 5–7). In the operculum, salt gland, and stingray rectal gland, junctions between transporting cells are present generally as doublets (Figs. 8–10 and references 45 and 20, respectively), although some single-stranded junctional areas may be present.[3] Junctional strands in the dogfish rectal gland average 3.5 and are also closely apposed (20). Moreover, all of these secretory cells exhibit a large ratio of junctional length to luminal surface area. The commonality in junctional architecture expressed by all of these hypertonic secretory epithelia suggests an underlying functional correlation which possibly may relate to the proposed conductive selectivity of the junctions toward ions and water and to the stability of the apical epithelial barrier. Further observations will be necessary to determine whether there will be a valid correlation between paracellular pathways and the structure of the zonula occludens for most, or all, chloride-secreting epithelia.

---

[1] Recent morphometric studies in rectal glands, which exhibit a similar pattern of junctional tortuosity, indicate that this parameter is indeed quite large amounting to 70 m of junction/cm^2 (19, 20).

[2] Rectal glands secrete a fluid that is isotonic; however, the secretion is NaCl-rich and is balanced osmotically in the plasma by urea retention.
[3] Although Sardet et al. (47) reported single strands between chloride cells in branchial epithelium, we have shown elsewhere (45) that doublets are sometimes hard to resolve, particularly when fracture planes undergo a transition from one cell to another across the junction, generating a strand and a continuous, but hard to resolve, groove (see Fig. 10). With this experience in mind, we interpret the image of the chloride cell–chloride cell junction in the gill (Fig. 9 c in reference 47) to be consistent with a doublet morphology, although additional freeze-fracture data are required to further substantiate this interpretation.

REFERENCES

1. Barry, P. H., J. M. Diamond, and E. M. Wright. 1971. The mechanism of cation permeation in rabbit gall-bladder. *J. Membr. Biol.* 4:358–394.
2. Bereiter-Hahn, J. 1976. Dimethylaminostyrylmethylpyridiniumiodine (DASPMI) as a fluorescent probe for mitochondria *in situ. Biochim. Biophys. Acta.* 423:1–14.
3. Boulpaep, E. L. 1971. Electrophysiological properties of the proximal tubule: importance of cellular and intercellular transport pathways. *In* Electrophysiology of Epithelial Cells, G. Giebisch, editor. F. K. Schattauer-Verlag, Stuttgart, Germany. 91–112.
4. Claude, P. 1978. Morphological factors influencing transepithelial permeability: A model for the resistance of the *zonula occludens. J. Membr. Biol.* 39:219–232.
5. Claude, P., and D. A. Goodenough. 1973. Fracture faces of *zonulae occludentes* from "tight" and "leaky" epithelia. *J. Cell Biol.* 58:390–400.
6. Degnan, K. J., K. J. Karnaky, Jr., and J. A. Zadunaisky. 1977. Active chloride transport in the *in vitro* opercular skin of a teleost (*Fundulus heteroclitus*), a gill-like epithelium rich in chloride cells. *J. Physiol. (Lond.)*. 27:155–191.
7. Degnan, K. J., and J. A. Zadunaisky. 1979. Open-circuit Na$^+$ and Cl$^-$ fluxes across isolated opercular epithelial from the teleost, *Fundulus heteroclitus. J. Physiol. (Lond.)*. 294:483–495.
8. Degnan, K. J., and J. A. Zadunaisky. 1980. Sodium and urea movements across the opercular epithelium: the effect of triaminopyrimidine (TAP) on the paracellular shunt pathway and ionic conductance. *J. Membr. Biol.* In press.
9. Degnan, K. J., and J. A. Zadunaisky. 1980. Ionic contributions to the potential and current across the opercular epithelium. *Am. J. Physiol.* 238:R231–R239.
10. Diamond, J. M. 1974. Tight and leaky junctions of epithelia: a perspective on kisses in the dark. *Fed. Proc.* 33:2220–2224.
11. Diamond, J. M. 1978. Channels in epithelial cell membranes and junctions. *Fed. Proc.* 37:2639–2644.
12. Diamond, J. M. 1979. Osmotic water flow in leaky epithelia. *J. Membr. Biol.* 51:195–216.
13. DiBona, D. R., and J. W. Mills. 1979. Distribution of Na$^+$-pump sites in transporting epithelia. *Fed. Proc.* 38:134–143.
14. Duffey, M. E., P. Silva, R. A. Frizzell, F. H. Epstein, and S. G. Schultz. 1978. Intracellular electrical potentials and chloride activities in the perfused rectal gland of *Squalus acanthias*: a report of preliminary data. *Bull. Mt. Desert Isl. Biol. Lab.* 18:73–74.
15. Dunel, S., and P. Laurent. 1973. Ultrastructure comparée de la pseudobranchie chez les téléostéens marins et d'eau douce. I. -L'epithelium pseudobranchial. *J. Microsc. (Paris.)*. 16:53–74.
16. Ellis, R. A., C. C. Goertemiller, Jr., and D. L. Stetson. 1977. Significance of extensive "leaky" cell junctions in the avian salt gland. *Nature (Lond.)*. 263:555–556.
17. Erlij, D. 1976. Solute transport across isolated epithelia. *Kidney Int.* 9:76–87.
18. Ernst, S. A., W. C. Dodson, and K. J. Karnaky, Jr. 1978. Structural diversity of *zonulae occludentes* in seawater-adapted killifish opercular epithelium. *J. Cell Biol.* 79(2, Pt. 2): 242a(Abstr.).
19. Ernst, S. A., S. R. Hootman, J. H. Schreiber, and C. V. Riddle. 1979. Structure of occluding junctions in the salt secreting epithelium of elasmobranch rectal gland. *J. Cell Biol.* 83(2, Pt. 2):83a(Abstr.).
20. Ernst, S. A., S. R. Hootman, J. H. Schreiber, and C. V. Riddle. 1980. Freeze-fracture and morphometric analysis of occluding junctions in rectal glands of elasmobranch fish. *J. Membr. Biol.* In press.
21. Ernst, S. A., and J. W. Mills. 1977. Basolateral plasma membrane localization of ouabain-sensitive sodium transport sites in the secretory epithelium of the avian salt gland. *J. Cell. Biol.* 75:74–94.
22. Ernst, S. A., and J. W. Mills. 1980. Autoradiographic localization of sodium pump sites in ion transporting epithelia with tritiated ouabain. *J. Histochem. Cytochem.* 28:72–77.
23. Ernst, S. A., C. V. Riddle, and K. J. Karnaky, Jr. 1980. Relationships between localization of Na$^+$-K$^+$-ATPase, cellular fine structure, and reabsorptive and secretory electrolyte transport. *In* Current Topics in Membranes and Transport. Vol. 13. E. Boulpaep, editor. Academic Press, Inc., New York. 355–385.
24. Eveloff, J., R. Kinne, E. Kinne-Saffran, H. Murer, P. Silva, F. H. Epstein, J. Stoff, and W. B. Kinter. 1978. Coupled sodium and chloride transport into plasma membrane vesicles

prepared from dogfish rectal gland. *Pflügers Arch. Eur. J. Physiol.* 378:87–92.
25. Field, M. 1978. Some speculations on the coupling between sodium and chloride transport processes in mammalian and teleost intestine. *In* Membrane Transport Processes. Vol. I. J. F. Hoffman, editor. Raven Press, New York. 277–292.
26. Frederiksen, O., K. Møllgard, and J. Rostgaard. 1979. Lack of correlation between transepithelial transport capacity and paracellular pathway ultrastructure in Alcian blue-treated rabbit gallbladders. *J. Cell Biol.* 83:383–392.
27. Frizzell, R. H., M. Field, and S. G. Schultz. 1979. Sodium-coupled chloride transport by epithelial tissues. *Am. J. Physiol.* 236:F1–F8.
28. Frizzell, R. A., and S. G. Schultz. 1972. Ionic conductances of extracellular shunt pathway in rabbit ileum. Influence of shunt on transmural sodium transport and electrical potential differences. *J. Gen. Physiol.* 59:313–346.
29. Frömter, E. 1972. The route of passive ion movement through the epithelium of *Necturus* gallbladder. *J. Membr. Biol.* 8:259–301.
30. Frömter, E., and J. Diamond. 1972. Route of passive ion permeation in epithelia. *Nat. New Biol.* 235:9–13.
31. Frömter, R., G. Rumrich, K. J. Ullrich. 1973. Phenomenologic description of Na, Cl and HCO$_3$ absorption from proximal tubules of the rat kidney. *Pflügers Arch. Eur. J. Physiol.* 343:189–220.
32. Helman, S. I., J. J. Grantham, and M. B. Burg. 1971. Effect of vasopressin on electrical resistance of renal cortical collecting tubules. *Am. J. Physiol.* 220:1825–1837.
33. Hootman, S. R., and C. W. Philpott. 1979. Ultracytochemical localization of Na$^+$, K$^+$-activated ATPase in chloride cells from the gills of a euryhaline teleost. *Anat. Rec.* 193:99–129.
34. Hootman, S. R., and C. W. Philpott. Accessory cells in teleost branchial epithelium. *Am. J. Physiol.* 238:R199–R206.
35. Karnaky, K. J., Jr. 1980. Ion-secreting epithelia: chloride cells in the head region of *Fundulus heteroclitus. Am. J. Physiol.* 238:R185–R198.
36. Karnaky, K. J., Jr., K. J. Degnan, and J. A. Zadunaisky. 1977. Chloride transport across isolated opercular epithelium of killifish: a membrane rich in chloride cells. *Science (Wash. D. C.)*. 195:203–205.
37. Karnaky, K. J., Jr., S. A. Ernst, and C. W. Philpott. 1976. Osmoregulation in euryhaline teleosts. I. Response of gill Na,K-ATPase, and chloride cell fine structure to various environments. *J. Cell Biol.* 70:144–156.
38. Karnaky, K. J., Jr., and W. B. Kinter. 1977. Killifish opercular skin: a flat epithelium with a high density of chloride cells. *J. Exp. Zool.* 199:355–364.
39. Karnaky, K. J., Jr., L. B. Kinter, W. B. Kinter, and C. E. Stirling. 1976. Teleost chloride cell. II. Autoradiographic localization of gill Na, K-ATPase in killifish (*Fundulus heteroclitus*) adapted to low and high salinity environments. *J. Cell Biol.* 80:157–177.
40. Maetz, J. 1971. Fish gills: mechanisms of salt transfer in fresh water and sea water. *Philos. Trans. R. Soc. Lond. B. Biol. Sci.* 262:209–249.
41. Malnic, G., and G. Giebisch. 1972. Some electrical properties of distal tubular epithelium in the rat. *Am. J. Physiol.* 223:797–808.
42. Martin, B. J., and C. W. Philpott. 1973. The adaptive response of the salt gland of adult mallard ducks to a salt water regime: an ultrastructural and tracer study. *J. Exp. Zool.* 186:111–122.
43. Moreno, J. H. 1975. Blockage of gallbladder tight junction cation-selective channels by 2,4,6-triaminopyrimidine (TAP). *J. Gen. Physiol.* 66:97–115.
44. Pricam, C., F. Humbert, A. Perrelet, and L. Orci. 1974. A freeze-etch study of the tight junctions of the rat kidney tubules. *Lab Invest.* 30:286–291.
45. Riddle, C. V., and S. A. Ernst. 1979. Structural simplicity of the *zonula occludens* in the electrolyte secreting epithelium of the avian salt gland. *J. Membr. Biol.* 45:21–35.
46. Sackin, H., and E. L. Boulpaep. 1975. Models of coupling of salt and water transport. Proximal tubular reabsorption in Necturus kidney. *J. Gen. Physiol.* 66:671–733.
47. Sardet, C., M. Pisam, and J. Maetz. 1979. The surface epithelium of teleostean fish gills. Cellular and junctional adaptations of the chloride cell in relation to salt adaptation. *J. Cell Biol.* 80:96–117.
48. Schultz, S. G. 1977. The role of paracellular pathways in isotonic fluid transport. *Yale J. Biol. Med.* 50:99–113.
49. Silva, P., R. Solomon, K. Spokes, and F. H. Epstein. 1977. Ouabain inhibition of gill Na-K-ATPase: relationship to active chloride transport. *J. Exp. Zool.* 199:419–426.
50. Silva, P., J. Stoff, M. Field, L. Fine, J. N. Forrest, and F. H. Epstein. 1978. Mechanism of active chloride secretion by shark rectal gland: role of Na-K-ATPase in chloride transport. *Am. J. Physiol.* 233:F298–F306.
51. Simionescu, N., and M. Simionescu. 1976. Galloylglucoses of low molecular weight as mordant in electron microscopy. *J. Cell Biol.* 70:608–621.
52. Stoff, J. S., P. Silva, M. Field, J. Forrest, A. Stevens, and F. H. Epstein. 1977. Cyclic AMP regulation of active chloride transport in the rectal gland of marine elasmobranchs. *J. Exp. Zool.* 199:443–448.
53. Van Lennep, E. W. 1968. Electron microscopic histochemical studies on salt-excreting glands in elasmobranchs and marine catfish. *J. Ultrastruct. Res.* 25:94–108.
54. Wright, E. M., A. P. Smulders, and J. McD. Tormey. 1972. The role of the lateral intercellular spaces and solute polarization effects in the passive flow of water across rabbit gallbladder. *J. Membr. Biol.* 7:198–219.